

Model Evaluation of Secondary Chemistry due to Disinfection of Indoor Air with Germicidal Ultraviolet Lamps

Zhe Peng,^{1*} Shelly L. Miller,² and Jose L. Jimenez^{1*}

¹ Cooperative Institute for Research in Environmental Sciences and Department of Chemistry, University of Colorado, Boulder, Colorado 80309, United States

² Department of Mechanical Engineering, University of Colorado, Boulder, Colorado 80309, United States

* **Corresponding authors:** Zhe Peng <zhe.peng@colorado.edu>; Jose L. Jimenez <jose.jimenez@colorado.edu>

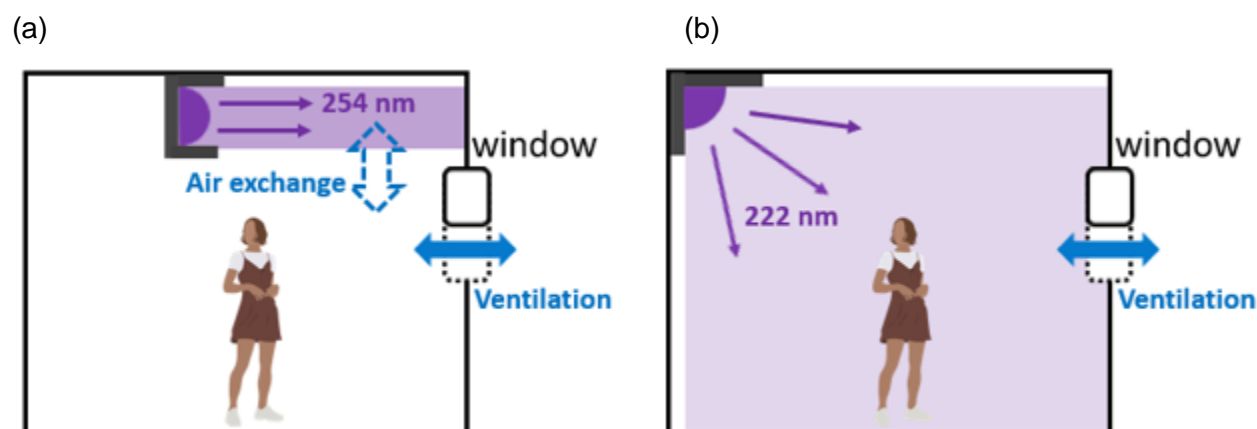
Abstract. The disinfection of air using Germicidal Ultraviolet light (GUV) is a long-standing technique, which has received increasing attention during the COVID-19 pandemic. GUV uses UVC lamps as its light source, which are known to inactivate microorganisms by damaging their genetic material. But they also initiate photochemistry in air. However, the impact of GUV on indoor air quality and chemistry has not been investigated in detail, to our knowledge. In this study, we model the chemistry initiated by GUV at 254 or 222 nm (“GUV254” or “GUV222”) in a typical room with typical indoor pollutant levels, and for different ventilation levels. GUV254 is irritating for skin and eyes, has an occupational exposure limit, and thus these fixtures typically irradiate a smaller volume near the ceiling, or inside ventilation ducts. In contrast, GUV222 is described by some as harmless to skin or eyes due to rapid absorption in a very thin external layer. Our analysis showed that GUV254 is able to significantly photolyze O₃, generating OH radicals, which initiates the oxidation of almost all indoor volatile organic compounds (VOCs). While secondary organic aerosol (SOA) can be formed as a product of VOC oxidation, most of the SOA in our case studies is produced through GUV-independent terpene ozonolysis. GUV254-induced SOA formation is of the order of 0.1-1 μg m⁻³. GUV222 with the same effective virus removal rate makes a smaller impact on indoor air quality at mid to high ventilation rates, mainly because of the significantly lower UV irradiance needed and thus substantially less efficient O₃ photolysis (for primary OH generation) than at 254 nm. GUV222 has a higher impact than GUV254 when ventilation is poor due to a small but significant photochemical production of O₃ at 222 nm, which does not happen with GUV254.

Keywords: ultraviolet germicidal irradiation; SARS-CoV-2; indoor air quality; photochemistry; ventilation; airborne disease transmission

36 **Synopsis:** Germicidal ultraviolet light initiates indoor oxidation chemistry, potentially forming
37 indoor air pollutants. The amount is not negligible and depends on both the wavelength of light
38 and the ventilation level.
39

Introduction

Germicidal ultraviolet light (GUV) has been employed to disinfect air in indoor spaces since the 1930s.¹ It has been shown to effectively limit the airborne transmission of infectious diseases, e.g., measles and tuberculosis.^{1–3} This is due to photon-induced dimerization of pyrimidines in the nucleic acids of airborne pathogens (and loss of their ability to replicate as a result). GUV fixtures use lamps that emit in the UVC range, most commonly at 254 nm (referred to hereinafter as “GUV254”).⁴ As 254 nm UV can cause skin and eye irritation on overexposure,⁵ GUV254 is usually applied near the ceiling, either inside an enclosed ceiling-mounted box, or irradiating the open air in the upper room (Figure 1a) or inside ventilation ducts. Recently, 222 nm UV has been shown to not only have strong capability of inactivating airborne viruses,⁶ but also is reported by some⁷ to be safer to humans (despite reports of the contrary),⁸ potentially allowing whole-room GUV applications (GUV222) (Fig. 1b). Ground-resting GUV-based air cleaners have also been commercialized, in which a fan continuously pulls air into a box and exposes it to UV light, from which the occupants are shielded.⁹



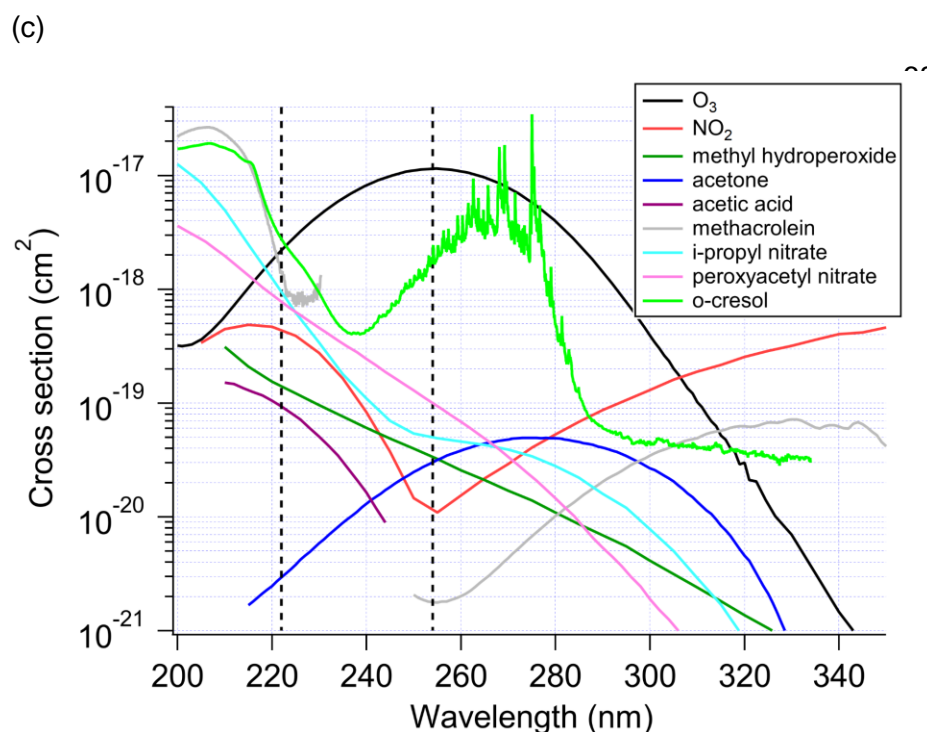


Figure 1.
Schematics of a
germicidal ultraviolet
air disinfection
system at (a) 254
nm and at (b) 222
nm in a room; (c)
absorption cross
sections of several
important gas-phase
species relevant to
this study (a
discontinuity in the
spectrum of

methacrolein is due to lack of data).

During the ongoing coronavirus disease 2019 (COVID-19) pandemic, UV has drawn renewed and increasing interest as a tool for airborne virus inactivation. Inhalation of airborne virus is widely accepted as the main transmission route of COVID-19,^{10–12} which explains the dominant indoor character of transmission.¹³ An important component of the transmission is due to superspreading events,¹⁴ which have been shown to be partly explained by shared-room airborne transmission.¹⁵ Much transmission also happens in close proximity due to short-range airborne transmission, but even in this situation a substantial fraction of the inhaled virus may come from well-mixed room air.^{16,17} As the pandemic continues, and with the possible appearance of new variants, there is a pressing need to remove viable severe acute respiratory syndrome coronavirus 2 (SARS-CoV-2) from indoor environments.³ Similar measures would be beneficial for other airborne diseases such as tuberculosis, measles, or a future pandemic virus.

Physical measures such as (natural and/or mechanical) ventilation and air filtration have been proven safe and effective.¹⁸ Nevertheless, mechanical ventilation and air filtration usually can remove airborne pathogens only at a few effective air changes per hour (ACH)¹⁹ and natural ventilation can be highly variable and impractical depending on weather, or when pollution, allergens or noise are present outdoors. When a high virus removal rate (e.g., >10 ACH) needs

to be ensured (e.g., in high-risk environments), GUV emerges as a practical and potentially cost-effective way to achieve it.^{3,18}

UVC light is known to generate strong oxidants (e.g., OH radicals, and sometimes also O₃ depending on the wavelengths used),²⁰ which can subsequently oxidize volatile organic compounds (VOCs) indoors and initiate organic radical chemistry in indoor air.^{21,22} Energetic UVC photons can also directly photolyze many VOCs, such as peroxides^{23,24} and carbonyls,^{25,26} and generate organic radicals. This radical chemistry is thought to lead to further oxidation of indoor VOCs and the formation of oxygenated VOCs (OVOCs) and secondary organic aerosol (SOA), both of which may have negative health effects.²⁷ Surveys of the concentration of total VOCs in the indoor environments range from ~0.1-4 mg m⁻³.²⁸⁻³⁰ Thus there is always a significant amount of VOC to react with any radicals and oxidants that are generated indoors, and any air cleaning technique that can create radicals and/or oxidants indoors have the potential to lead to secondary chemistry.²⁷ Very few studies on this topic have been conducted with state-of-the-art measurements or models. Recently, air cleaning devices based on chemistry induced by UV light (photocatalysis and OH generation, but not GUV), often also marketed as suitable for air disinfection, have been experimentally shown to produce significant amounts of OVOCs and SOA.^{31,32}

Despite the potential of GUV to cause secondary chemistry, to our knowledge this topic has not been studied in detail to date. Some studies of GUV inactivation effectiveness have included measurements of ozone, to assess whether any was generated.⁹ These studies report no production of ozone when mercury vapor lamps coated to limit emission from wavelengths nearer to the ozone generating wavelength of 185 nm are used, as expected. However, some uncoated or improperly-coated lamps are commercially available, so ozone production can be a problem in some cases. In this study, we perform a first evaluation of the impacts of GUV at both 254 nm (assuming properly-coated lamps) and 222 nm on indoor air quality, using a model. The amounts of OVOC and SOA that can be formed in typical indoor environments are investigated.

Materials and Methods

We include the photochemistry due to GUV and subsequent radical, oxidation, and SOA formation chemistries. Given the complexity of the composition of indoor air, we simplify both

the chemical species present indoors and the reaction scheme, while keeping them consistent with the state-of-the-art knowledge for indoor air. Surface reactions are neglected but could be important, and should be investigated in future studies.

The chemical mechanism for this study is a combination of the inorganic radical chemistry in an oxidation flow reactor (OFR)^{20,33,34} and part of the Regional Atmospheric Chemistry Mechanism (RACM)³⁵ relevant to this study. The OFR also employs UVC lamps, with the explicit purpose of generating radicals that initiate oxidation reactions. OFR are used extensively in atmospheric chemistry research. A common OFR operation mode (“OFR254”) uses 254 nm UV light from filtered mercury lamps to photolyze O₃, through which O(¹D) is generated, which subsequently reacts with water vapor to form OH.^{20,33} OFR254 uses the same type of lamps as GUV254 and thus OH is expected to form through the same chemistry. Therefore, all reactions of this inorganic radical chemistry are adopted.²⁰ For organic chemistry, the relevant reactions in RACM are adopted. Among major relevant (lumped) species are HC8 (alkanes, alcohols, and esters with relatively fast reaction rate with OH), LIM (limonene), KET (ketones), ALD (aldehydes), OP2 (higher organic peroxides), and ACO3 (acylperoxy radicals). Section S1 in the Supp. Info. provides more details of the adaptation of RACM to this study, and Table S1 lists all organic reactions modeled in the present work. All photolysis cross sections are adopted from refs 36,37 when available, otherwise estimated from those of molecules containing the same functional groups according to the framework of Peng et al.³⁸ All quantum efficiencies for reactant photodissociation except those with available data in refs 36,37 are assumed to be 1, given the high photon energies involved. For GUV222, the photolysis frequencies are calculated using the light flux at that wavelength. The chemical mechanisms are run within the open-source KinSim chemical kinetics simulator,³⁹ and are made available in the Supp. Info. and at the KinSim cases page.⁴⁰ We perform all simulations until a steady state is reached.

We investigate a typical indoor space with representative indoor and urban outdoor air concentrations from the literature, as shown in Table S2. The atmospheric pressure and temperature in the room are assumed to be 1 atm and 295 K, respectively, with a relative humidity of 37% (water vapor mixing ratio of 1%), and initial NO, HONO, NO₂, and O₃ concentrations of 1, 5, 10, and 10 ppbv, respectively. The initial concentrations of most VOCs are estimated based on the compilation of McDonald et al.,⁴¹ with the total VOC concentration assumed to be 1.7 mg m⁻³, a typical value for US indoor spaces.²⁸ Section S2 details how some individual species are lumped to enable combining the inventory of McDonald et al.⁴¹ with the

chemical reaction scheme of this study and how the fraction of each (lumped) species in the total VOC is estimated. The only exceptions to this initial VOC concentration estimation are that we assign higher concentrations of 300 ppb to acetone as measured by Price et al.³⁰ and of 2 ppm to formaldehyde per ref 28.

The 254 nm GUV fixture in our simulations is based on the AeroMed LEXUS L2.1 Open.⁴² The space irradiated by this device is 45 m³, and is placed in a room of 300 m³ (volume of a typical classroom), thus the irradiated volume is 15% of the volume of the room, consistent with refs 43,44. The model for 254 nm GUV has two compartments (“boxes”), one for the irradiated zone and the other for the rest of the room, while that for 222 nm GUV has only one box. For the GUV254 case we set an air exchange rate for the irradiated zone at 240 h⁻¹ (with the unirradiated zone),⁴⁵ which leads to a modeled effective GUV virus removal rate for the whole room of ~30 h⁻¹ (equivalent ACH) using a SARS-CoV-2 UV inactivation rate of 0.79 cm²/mJ.⁶ Such an equivalent ACH is representative of well-designed indoor GUV applications.^{3,43,44} Air within a modeled indoor air compartment is assumed to be well mixed. Although highly reactive radicals (e.g., OH) may not travel far from the irradiated zone due to short lifetimes,⁴⁶ their concentrations can still be averaged over the entire unirradiated space because of their low concentrations and thus the low importance of self- and cross-reactions in their fates. Based on the UV inactivation rate constants at 222 nm for SARS-CoV-2,^{6,7} the UV intensity of the 222 nm fixture is adjusted such that this fixture also provides the same whole-room effective virus removal rate as for GUV254 (see Section S3 for the details of UV intensity calculation). Three levels of ventilation, i.e., a representative residential level (0.3 ACH, “low ventilation”),⁴⁷ a representative commercial level (3 ACH, “medium ventilation”),¹⁹ and a representative medical level (9 ACH, “high ventilation”)³ are simulated in this study. Indoor VOC emissions are set such that all VOC concentrations remain at their literature-constrained initial values at low ventilation without chemistry occurring. We assume no NO_x or O₃ emissions indoors, and 5 ppb NO, 20 ppb NO₂, 40 ppb O₃ outdoors. No VOC is assumed to be present in outdoor air, as outdoor VOC levels are typically much lower than indoor ones.^{29,30} The O₃ surface loss rate in the absence of chemistry is set to 2.8 h⁻¹, which is typical of residences⁴⁸ and is known to be sensitive to occupancy and the indoor surfaces present. To test COVID-19 infection risk in different situations, we assume the presence of an infector shedding SARS-CoV-2 at 16 quanta h⁻¹ (roughly for light exercise while speaking 50% time),⁴⁹ which is consistent or lower than values constrained for literature superspreading events.¹⁵ A quantum is an infectious dose, that if inhaled by a susceptible person, will lead to a probability of infection of 1-1/e.^{15,50} The rate of

SARS-CoV-2 loss apart from ventilation and GUV (i.e., due to intrinsic loss of infectivity, aerosol deposition etc.) is assumed to be 1 h^{-1} .

Results and Discussion

Disinfection. Figure 2 shows the amount of SARS-CoV-2 present in the room to be consistent with the steady-state prediction. In the absence of GUV, the emission rate of SARS-CoV-2 is 16 quanta h^{-1} , and its total loss rate 1.3 h^{-1} (0.3 h^{-1} from ventilation and 1 h^{-1} from decay and deposition) for the low-ventilation case. The steady state SARS-CoV-2 quantity in the entire room is 12.3 quanta. Similarly, it is lowered to 4 and 1.6 quanta by increasing the ventilation rate to 3 and 9 ACH, respectively. When a GUV fixture with a whole-room virus removal rate of $\sim 30 \text{ h}^{-1}$ is applied, the SARS-CoV-2 quantity decreases to ~ 0.6 , ~ 0.5 , and ~ 0.4 quanta in the low-, medium-, and high-ventilation cases, respectively. The relative impact of GUV is higher at low ventilation, as expected.

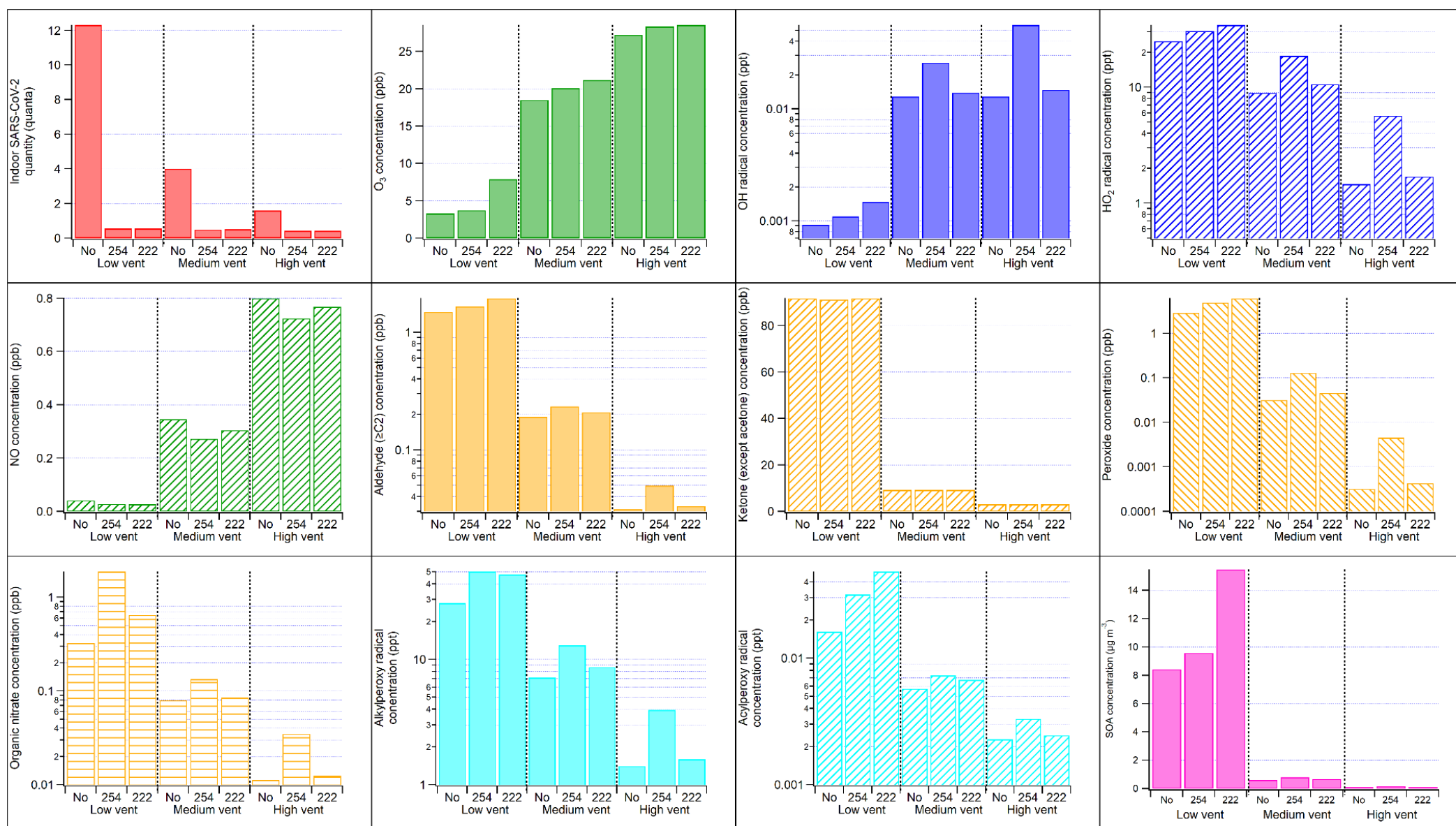


Figure 2. Final quantity/concentration of the main (types of) species of interest in this study under different GUV and ventilation conditions. In the GUV254 cases, the volume-weighted average concentrations for the whole room are shown. The stable chemical species concentrations are similar between the irradiated and unirradiated zones, while the radical and SARS-CoV-2 concentrations in the unirradiated zone can be significantly lower and higher, respectively (Table S3). Note that some panels use log scale for concentrations while other panels use linear scale. SOA is assumed to have a molar weight of 200 g mol⁻¹.

The total quantity of SARS-CoV-2 does not directly reflect its infection risk, which also depends on the volume of the room and the inhalation by susceptible occupants. For an occupant with a breathing rate of $0.5 \text{ m}^3 \text{ h}^{-1}$ (typical for light physical activities)⁵¹ present in the 300 m^3 room with low ventilation and no GUV fixture for 1 h, ~ 0.02 quantum is inhaled. This corresponds to an infection probability of $\sim 2\%$, since the infection probability is approximately equal to the inhaled quanta if the latter is small.⁵² For the cases studied in this work, infection risk is reduced by $x \sim 3$ by medium ventilation, and by a factor of ~ 22 (~ 8) when adding GUV to a low (medium) ventilation situation. When adding GUV to a high ventilation situation, the risk reduction is less than a factor of 4.

Secondary Chemistry. For chemical species in the room, ventilation alone (without GUV) can make some difference (Fig. 2). The differences in O_3 , NO, and ketone concentrations are largely due to these species being ventilated in or out. For other chemical species, secondary chemical processes also play a role. OH radicals can form even without UV, i.e., from limonene ozonolysis. As a result, OH radicals are higher at medium and high ventilation, which introduces more O_3 from outdoors than at low ventilation. OH concentration at high ventilation is not higher than medium ventilation because high ventilation also dilutes limonene concentration indoors, reducing the overall limonene- O_3 reaction rate. HO_2 radicals are lower at higher ventilation because of higher NO being ventilated into the room, which reacts with HO_2 . All other organic radicals and stable products shown in Fig. 2 (including SOA) have higher concentrations in the low-ventilation case due to higher VOC concentrations.

When GUV254 is employed, although the concentration of photolyzable O_3 remains relatively stable due to much stronger replenishment from outdoor air ventilation than photolytic destruction, the chemistry is significantly altered by UV (Fig. 2). The fundamental cause of this change is OH production from O_3 photolysis under 254 nm UV irradiation.²⁰ OH concentrations in the GUV254 cases are approximately a factor of 1.2-5 and 3-20 times those in the corresponding no-UV cases for the whole room average and for the irradiated zone, respectively. The difference in the higher-ventilation cases is larger, due to more O_3 in the room from outside air (Fig. 2 and Table S3). OH in the higher-ventilation cases is similar to daytime outdoor urban levels.⁵³ This OH level is high enough to drive substantial oxidation of VOCs, production of other radicals (e.g., HO_2 and organic peroxy radicals (RO_2)), and SOA formation. Organic peroxides (including hydroperoxides), carbonyls (aldehydes (excluding formaldehyde) and ketones (excluding acetone)), and organic nitrates (including peroxy nitrates) are among

common VOC oxidation products and all have ~10% to several-fold concentration increases (Fig. 2). The exceptions are ketones (excluding acetone), whose production is dominated in the model by UV-independent limonene ozonolysis (Fig. 2). Doubling RH significantly increases OH concentration, but changes of product species are within 10% of the base RH results, likely due to non-linear buffering from the reaction scheme (not shown). The exceptions are ketones, which are relatively unreactive and dominated in the model by the chemistry-independent acetone emission and its dilution by ventilation (Fig. 2). In addition to VOC oxidation by OH, radicals (OH, HO₂, and RO₂) are also produced by active photolysis of carbonyls and peroxides at 254 nm, where both strongly absorb (Fig. 1c).

Due to higher peroxy radical concentrations, NO is lowered to ~30 ppt at low ventilation (Fig. 2). Such a low NO concentration leads to reactions of RO₂ with both HO₂ and NO being important, as estimated per Peng et al.⁵⁴ They both account for nearly half of the RO₂ bimolecular loss in the irradiated space (Fig. S1). Also, without fast RO₂+NO, RO₂ lifetime is sufficiently long for unimolecular reactions of RO₂ to occur (Fig. S1) as observed previously indoors for similar conditions,⁵⁵ although RACM does not include these reactions. In the higher ventilation cases, NO, though still consumed by the photochemistry, is much higher due to a stronger replenishment from outdoor air and can dominate the RO₂ bimolecular fate (Fig. S1).

SOA formation is estimated from the consumption of individual VOCs and SOA mass yields from the literature (Table S4). Significant SOA production (~8 µg m⁻³ at low ventilation) occurs even with GUV irradiation, through limonene ozonolysis, as this reaction has a high SOA yield (20%). In the GUV254 cases, both limonene ozonolysis and VOC oxidation by OH contribute to SOA. Nevertheless, the enhanced contribution from OH oxidation of VOC under GUV irradiation is a fraction of SOA formed in the no-UV cases (Fig. 2), because of a large fraction of total VOC present being species too small to form SOA through oxidation (e.g., ethanol, acetone, and isopropyl alcohol). The overall SOA mass yield from total VOC is of the order of 0.1%. Given that 1.5 mg m⁻³ of total VOCs (excluding limonene) are present, that leads to ~1.2 µg m⁻³ due to GUV254. The enhancement of SOA formation by OH oxidation relative to the no-UV cases (mainly from VOC ozonolysis) decreases with ventilation, as VOC concentrations are lowered by higher ventilation (Fig. 2). The SOA precursors and mechanism used in this work are likely incomplete, given the incomplete scientific understanding of this topic.⁵⁶

Due to the fast air exchange between the GUV254 irradiated and unirradiated spaces, the concentrations of stable species are similar between these two spaces (Table S3). In contrast, radicals are more rapidly consumed in the unirradiated space than supplied by the transport from the irradiated space, and thus have much lower concentrations (up to >1 order of magnitude for highly reactive ones such as OH and acylperoxy) in the unirradiated space than in the irradiated space.

The GUV222 cases in this study assume irradiation of the entire room volume (Fig. 1b). Also, photons at 222 nm are able to photolyze O₂ and produce O₃, albeit at a small rate, leading to higher O₃ in all cases relative to GUV254. The amounts of organic products formed in the medium- and high-ventilation (low-ventilation) cases are lower (higher) than in the unirradiated zone in the GUV254 cases (Fig. 2).

At medium and high ventilation rates, the main O₃ source in the GUV222 cases is still outdoor O₃ through ventilation. Despite the slightly stronger O₃ production due to O₂ photolysis, the product formation enhancement in these GUV222 cases is much smaller than in the corresponding GUV254 cases (Fig. 2). These results indicate a very weak OH-initiated VOC oxidation in these cases on top of the VOC ozonolysis chemistry that is active in the no-UV cases.

This difference from the active photochemistry in the GUV254 cases can be attributed to several factors. First, the UV irradiance of the 222 nm fixture is significantly lower, even in terms of the number of photons emitted per unit time. 222 nm photons are ~40% more efficient in inactivating SARS-CoV-2 than 254 nm photons.⁶ In addition the latter cannot be used in the most efficient fashion. Due to the need to protect humans from irradiation, all photons are concentrated in the small irradiated zone (15% of the room volume). Because of the limitation of transport of virus-containing aerosol from the unirradiated zone, the steady-state infectious virus concentration is ~70% lower than in the unirradiated zone, where the infector and the susceptible individuals are present (Table S3). Even with the same per-photon virus inactivation efficiency, GUV254 needs about 3 times the photons for GUV222 to reach the same effective GUV virus removal rate for the occupied unirradiated space. Furthermore, the first step of OH photochemical production is O₃ photolysis, whose corresponding absorption at 222 nm is about ~5 times lower than at 254 nm (Fig. 1c). Simple carbonyl compounds, the most abundant OVOCs in this study, also absorb much less efficiently at 222 nm than at 254 nm (Fig. 1c),

further reducing radical production. Although other products, such as peroxides and conjugated carbonyl species, can have stronger absorption at 222 nm, their relatively low concentrations (~1 ppb or lower vs. hundreds of ppb of ketones) limit their relative contributions to the radical budget.

Because of the small direct production of O_3 by the GUV222 lights, O_3 in the GUV222 low-ventilation case is substantially less depleted by limonene ozonolysis than for GUV254. As a result, compared to GUV254 SOA formation through limonene ozonolysis is substantially stronger and OH concentration is also higher (Fig. 2) despite a lower cross section of O_3 photolysis at 222 nm. Other gas-phase stable organic products have comparable concentrations with those in the GUV254 case.

Implications. We have shown that GUV disinfection can induce active photochemistry producing OVOCs and SOA in typical indoor environments. Under the conditions simulated here, these products do not necessarily have significant negative effects on human health because of their relatively low concentrations. Among the VOCs (including OVOCs) modeled in this study, only formaldehyde has a concentration exceeding the Minimal Risk Level (MRL) recommended by the CDC⁵⁷ due to strong indoor emissions. However, only a very limited number of species were explicitly modeled in this study, particularly aldehydes, whose toxicity is generally high. Future studies with higher chemical speciation are needed to better assess the toxicity of gas-phase products. In polluted indoor spaces and/or outdoor atmospheric environments, the indoor concentrations of the VOCs of interest can be much higher,²⁴ while the GUV-induced photochemistry can still be active (see Sections S4 and S5 for more detail). In this case, OVOC products might exceed the MRLs and SOA formation might reach tens of $\mu g m^{-3}$.

The risk of GUV254 due to secondary photochemical products is not negligible but also not dominant under typical indoor conditions. The risk for GUV222 appears to be substantially lower when ventilation is not poor, but comparable or slightly higher in case of poor ventilation. We note that many indoor environments, in particular homes and schools, have ventilation rates similar to the definition of “poor” in this paper, even in high-income countries. If GUV222 is confirmed to be safe for direct human exposure, it would have an advantage over GUV254 at mid to high ventilation rates in terms of indoor chemistry, in addition to more efficient air disinfection. When 254 nm fixtures are used, a strong air exchange between the irradiated and unirradiated zones (e.g., by fans) is preferable, as recommended by the CDC/NIOSH.⁵⁸ It can

lower the UV irradiance needed for a given virus inactivation rate,⁵⁹ and hence limit the induced photochemistry. Good ventilation can not only remove airborne pathogens, but also limit the production of secondary indoor pollutants, and is thus also recommended when outdoor air is relatively clean.^{19,60} Similarly, particulate air filtration is also recommended as it removes both virus-containing aerosol, indoor-formed SOA, and particulate pollution from other indoor and outdoor sources. Gas filtration with sorbent materials such as activated carbon is also useful for reducing VOC, NO_x and ozone levels indoors.^{61,62} The findings of this study are limited due to modeling assumptions, e.g., the simplified chemical mechanism, limited data on photolysis parameters in the UVC range (particularly the quantum yields of aromatics), the assumed indoor and outdoor air pollutant compositions, uncertainties over precursors and yields of SOA formation, and surface reactions, which are still uncertain and/or variable. Experimental studies in both simplified laboratory settings and real indoor conditions are needed to fully constrain the impacts of GUV in indoor chemistry.

Acknowledgements

ZP and JLJ were partially supported by the CIRES Innovative Research Program. We thank Vito Ilacqua, Zachary Finewax, Donald Milton, and Edward Nardell for valuable discussions.

References

- (1) Wells, W. F.; Wells, M. W.; Wilder, T. S. The Environmental Control of Epidemic Contagion. I. *An epidemiologic study of radiant disinfection of air in day schools* *Am J Hyg* **1942**, *35*, 97–121.
- (2) Riley, R. L.; Mills, C. C.; O'grady, F.; Sultan, L. U.; Wittstadt, F.; Shivpuri, D. N. Infectiousness of Air from a Tuberculosis Ward. Ultraviolet Irradiation of Infected Air: Comparative Infectiousness of Different Patients. *Am. Rev. Respir. Dis.* **1962**, *85*, 511–525.
- (3) Nardell, E. A. Air Disinfection for Airborne Infection Control with a Focus on COVID-19: Why Germicidal UV Is Essential. *Photochem. Photobiol.* **2021**, *97* (3), 493–497.
- (4) Riley, R. L.; Nardell, E. A. Clearing the Air: The Theory and Application of Ultraviolet Air Disinfection. *American Review of Respiratory Disease*. 1989, pp 1832–1832. <https://doi.org/10.1164/ajrccm/140.6.1832b>.
- (5) Zaffina, S.; Camisa, V.; Lembo, M.; Vinci, M. R.; Tucci, M. G.; Borra, M.; Napolitano, A.; Cannata, V. Accidental Exposure to UV Radiation Produced by Germicidal Lamp: Case Report and Risk Assessment. *Photochem. Photobiol.* **2012**, *88* (4), 1001–1004.
- (6) Ma, B.; Gundy, P. M.; Gerba, C. P.; Sobsey, M. D.; Linden, K. G. UV Inactivation of SARS-CoV-2 across the UVC Spectrum: KrCl* Excimer, Mercury-Vapor, and LED Sources. *Appl. Environ. Microbiol.* **2021**. <https://doi.org/10.1128/AEM.01532-21>.

- (7) Buonanno, M.; Welch, D.; Shuryak, I.; Brenner, D. J. Far-UVC Light (222 Nm) Efficiently and Safely Inactivates Airborne Human Coronaviruses. *Sci. Rep.* **2020**, *10* (1), 10285.
- (8) Ong, Q.; Wee, W.; Cruz, J. D.; Ronnie Teo, J. W.; Han, W. 222-Nm Far UVC Exposure Results in DNA Damage and Transcriptional Changes to Mammalian Cells. *bioRxiv*, 2022, 2022.02.22.481471. <https://doi.org/10.1101/2022.02.22.481471>.
- (9) Kujundzic, E.; Matalak, F.; Howard, C. J.; Hernandez, M.; Miller, S. L. UV Air Cleaners and Upper-Room Air Ultraviolet Germicidal Irradiation for Controlling Airborne Bacteria and Fungal Spores. *J. Occup. Environ. Hyg.* **2006**, *3* (10), 536–546.
- (10) Wang, C. C.; Prather, K. A.; Sznitman, J.; Jimenez, J. L.; Lakdawala, S. S.; Tufekci, Z.; Marr, L. C. Airborne Transmission of Respiratory Viruses. *Science* **2021**, *373* (6558), eabd9149.
- (11) Greenhalgh, T.; Jimenez, J. L.; Prather, K. A.; Tufekci, Z.; Fisman, D.; Schooley, R. Ten Scientific Reasons in Support of Airborne Transmission of SARS-CoV-2. *Lancet* **2021**. [https://doi.org/10.1016/S0140-6736\(21\)00869-2](https://doi.org/10.1016/S0140-6736(21)00869-2).
- (12) Klompas, M.; Milton, D. K.; Rhee, C.; Baker, M. A.; Leekha, S. Current Insights Into Respiratory Virus Transmission and Potential Implications for Infection Control Programs : A Narrative Review. *Ann. Intern. Med.* **2021**, *174* (12), 1710–1718.
- (13) Qian, H.; Miao, T.; Liu, L.; Zheng, X.; Luo, D.; Li, Y. Indoor Transmission of SARS-CoV-2. *Indoor Air* **2020**, in press.
- (14) Adam, D. C.; Wu, P.; Wong, J. Y.; Lau, E. H. Y.; Tsang, T. K.; Cauchemez, S.; Leung, G. M.; Cowling, B. J. Clustering and Superspreading Potential of SARS-CoV-2 Infections in Hong Kong. *Nat. Med.* **2020**, *26* (11), 1714–1719.
- (15) Peng, Z.; Rojas, A. L. P.; Kropff, E.; Bahnfleth, W.; Buonanno, G.; Dancer, S. J.; Kurnitski, J.; Li, Y.; Loomans, M. G. L. C.; Marr, L. C.; Morawska, L.; Nazaroff, W.; Noakes, C.; Querol, X.; Sekhar, C.; Tellier, R.; Greenhalgh, T.; Bourouiba, L.; Boerstra, A.; Tang, J. W.; Miller, S. L.; Jimenez, J. L. Practical Indicators for Risk of Airborne Transmission in Shared Indoor Environments and Their Application to COVID-19 Outbreaks. *Environ. Sci. Technol.* **2022**, *56* (2), 1125–1137.
- (16) Li, Y.; Cheng, P.; Jia, W. Poor Ventilation Worsens Short-Range Airborne Transmission of Respiratory Infection. *Indoor Air* **2022**, *32* (1), e12946.
- (17) Jimenez, J. L.; Peng, Z.; Pagonis, D. Systematic Way to Understand and Classify the Shared-Room Airborne Transmission Risk of Indoor Spaces. *Indoor Air* **2022**, *32* (5), e13025.
- (18) Morawska, L.; Allen, J.; Bahnfleth, W.; Bluyssen, P. M.; Boerstra, A.; Buonanno, G.; Cao, J.; Dancer, S. J.; Floto, A.; Franchimon, F.; Greenhalgh, T.; Haworth, C.; Hogeling, J.; Isaxon, C.; Jimenez, J. L.; Kurnitski, J.; Li, Y.; Loomans, M.; Marks, G.; Marr, L. C.; Mazzearella, L.; Melikov, A. K.; Miller, S.; Milton, D. K.; Nazaroff, W.; Nielsen, P. V.; Noakes, C.; Peccia, J.; Prather, K.; Querol, X.; Sekhar, C.; Seppänen, O.; Tanabe, S.-I.; Tang, J. W.; Tellier, R.; Tham, K. W.; Wargocki, P.; Wierzbicka, A.; Yao, M. A Paradigm Shift to Combat Indoor Respiratory Infection. *Science* **2021**, *372* (6543), 689–691.
- (19) ASHRAE. *Ventilation for Acceptable Indoor Air Quality: ANSI/ASHRAE Standard 62.1-2019*; ANSI/ASHRAE, 2019.
- (20) Peng, Z.; Jimenez, J. L. Radical Chemistry in Oxidation Flow Reactors for Atmospheric Chemistry Research. *Chem. Soc. Rev.* **2020**, *49* (9), 2570–2616.
- (21) Atkinson, R.; Arey, J. Atmospheric Degradation of Volatile Organic Compounds. *Chem. Rev.* **2003**, *103* (12), 4605–4638.
- (22) Ziemann, P. J.; Atkinson, R. Kinetics, Products, and Mechanisms of Secondary Organic Aerosol Formation. *Chem. Soc. Rev.* **2012**, *41* (19), 6582–6605.
- (23) Blitz, M. A.; Heard, D. E.; Pilling, M. J. Wavelength Dependent Photodissociation of CH₃OOH: Quantum Yields for CH₃O and OH, and Measurement of the OH+ CH₃OOH Rate Coefficient. *J. Photochem. Photobiol. A Chem.* **2005**, *176* (1-3), 107–113.

- (24) Vaghjiani, G. L.; Ravishankara, A. R. Photodissociation of H₂O₂ and CH₃OOH at 248 Nm and 298 K: Quantum Yields for OH, O(3P) and H(2S). *J. Chem. Phys.* **1990**, 92 (2), 996–1003.
- (25) Link, M. F.; Farmer, D. K.; Berg, T.; Flocke, F.; Ravishankara, A. R. Measuring Photodissociation Product Quantum Yields Using Chemical Ionization Mass Spectrometry: A Case Study with Ketones. *J. Phys. Chem. A* **2021**, 125 (31), 6836–6844.
- (26) Rajakumar, B.; Gierczak, T.; Flad, J. E.; Ravishankara, A. R.; Burkholder, J. B. The CH₃CO Quantum Yield in the 248 Nm Photolysis of Acetone, Methyl Ethyl Ketone, and Biacetyl. *J. Photochem. Photobiol. A Chem.* **2008**, 199 (2-3), 336–344.
- (27) Collins, D. B.; Farmer, D. K. Unintended Consequences of Air Cleaning Chemistry. *Environ. Sci. Technol.* **2021**. <https://doi.org/10.1021/acs.est.1c02582>.
- (28) Logue, J. M.; McKone, T. E.; Sherman, M. H.; Singer, B. C. Hazard Assessment of Chemical Air Contaminants Measured in Residences. *Indoor Air* **2011**, 21 (2), 92–109.
- (29) Mattila, J. M.; Arata, C.; Abeleira, A.; Zhou, Y.; Wang, C.; Katz, E. F.; Goldstein, A. H.; Abbatt, J. P. D.; DeCarlo, P. F.; Vance, M. E.; Farmer, D. K. Contrasting Chemical Complexity and the Reactive Organic Carbon Budget of Indoor and Outdoor Air. *Environmental Science & Technology*. 2022, pp 109–118. <https://doi.org/10.1021/acs.est.1c03915>.
- (30) Price, D. J.; Day, D. A.; Pagonis, D.; Stark, H.; Algrim, L. B.; Handschy, A. V.; Liu, S.; Krechmer, J. E.; Miller, S. L.; Hunter, J. F.; de Gouw, J. A.; Ziemann, P. J.; Jimenez, J. L. Budgets of Organic Carbon Composition and Oxidation in Indoor Air. *Environ. Sci. Technol.* **2019**. <https://doi.org/10.1021/acs.est.9b04689>.
- (31) Ye, Q.; Krechmer, J. E.; Shutter, J. D.; Barber, V. P.; Li, Y.; Helstrom, E.; Franco, L. J.; Cox, J. L.; Hrdina, A. I. H.; Goss, M. B.; Tahsini, N.; Canagaratna, M.; Keutsch, F. N.; Kroll, J. H. Real-Time Laboratory Measurements of VOC Emissions, Removal Rates, and Byproduct Formation from Consumer-Grade Oxidation-Based Air Cleaners. *Environmental Science & Technology Letters* **2021**. <https://doi.org/10.1021/acs.estlett.1c00773>.
- (32) Joo, T.; Rivera-Rios, J. C.; Alvarado-Velez, D.; Westgate, S.; Lee Ng, N. Formation of Oxidized Gases and Secondary Organic Aerosol from a Commercial Oxidant-Generating Electronic Air Cleaner. *Environmental Science & Technology Letters* **2021**. <https://doi.org/10.1021/acs.estlett.1c00416>.
- (33) Peng, Z.; Day, D. A.; Stark, H.; Li, R.; Lee-Taylor, J.; Palm, B. B.; Brune, W. H.; Jimenez, J. L. HO_x Radical Chemistry in Oxidation Flow Reactors with Low-Pressure Mercury Lamps Systematically Examined by Modeling. *Atmospheric Measurement Techniques* **2015**, 8 (11), 4863–4890.
- (34) Peng, Z.; Jimenez, J. L. Modeling of the Chemistry in Oxidation Flow Reactors with High Initial NO. *Atmos. Chem. Phys.* **2017**, 17 (19), 11991–12010.
- (35) Stockwell, W. R.; Kirchner, F.; Kuhn, M.; Seefeld, S. A New Mechanism for Regional Atmospheric Chemistry Modeling. *J. Geophys. Res.* **1997**, 102 (D22), 25847–25879.
- (36) Burkholder, J. B.; Sander, S. P.; Abbatt, J.; Barker, J. R.; Huie, R. E.; Kolb, C. E.; Kurylo, M. J.; Orkin, V. L.; Wilmouth, D. M.; Wine, P. H. *Chemical Kinetics and Photochemical Data for Use in Atmospheric Studies: Evaluation Number 18*; Jet Propulsion Laboratory: Pasadena, CA, USA, 2015.
- (37) Keller-Rudek, H.; Moortgat, G. K.; Sander, R.; Sörensen, R. *The MPI-Mainz UV/VIS Spectral Atlas of Gaseous Molecules of Atmospheric Interest*. http://satellite.mpic.de/spectral_atlas (accessed 2022-02-10).
- (38) Peng, Z.; Lee-Taylor, J.; Stark, H.; Orlando, J. J.; Aumont, B.; Jimenez, J. L. Evolution of OH Reactivity in NO-Free Volatile Organic Compound Photooxidation Investigated by the Fully Explicit GECKO-A Model. *Atmos. Chem. Phys.* **2021**, 21 (19), 14649–14669.
- (39) Peng, Z.; Jimenez, J. L. KinSim: A Research-Grade, User-Friendly, Visual Kinetics Simulator for Chemical-Kinetics and Environmental-Chemistry Teaching. *J. Chem. Educ.*

- 2019, 96 (4), 806–811.
- (40) Downloadable KinSim cases and mechanisms. Google Docs.
https://docs.google.com/document/d/10OuUMtMGJsh90cQ3p4Y_oiKQdPRHYQnxKQr2_I62Kx0 (accessed 2022-07-31).
- (41) McDonald, B. C.; de Gouw, J. A.; Gilman, J. B.; Jathar, S. H.; Akherati, A.; Cappa, C. D.; Jimenez, J. L.; Lee-Taylor, J.; Hayes, P. L.; McKeen, S. A.; Cui, Y. Y.; Kim, S.-W.; Gentner, D. R.; Isaacman-VanWertz, G.; Goldstein, A. H.; Harley, R. A.; Frost, G. J.; Roberts, J. M.; Ryerson, T. B.; Trainer, M. Volatile Chemical Products Emerging as Largest Petrochemical Source of Urban Organic Emissions. *Science* **2018**, 359 (6377), 760–764.
- (42) Upper room germicidal ultraviolet fixtures. AeroMed Technologies.
<https://aeromed.com/product/upper-room-guv-fixtures/> (accessed 2022-02-21).
- (43) Xu, P.; Kujundzic, E.; Peccia, J.; Schafer, M. P.; Moss, G.; Hernandez, M.; Miller, S. L. Impact of Environmental Factors on Efficacy of Upper-Room Air Ultraviolet Germicidal Irradiation for Inactivating Airborne Mycobacteria. *Environ. Sci. Technol.* **2005**, 39 (24), 9656–9664.
- (44) Xu, P.; Peccia, J.; Fabian, P.; Martyny, J. W.; Fennelly, K. P.; Hernandez, M.; Miller, S. L. Efficacy of Ultraviolet Germicidal Irradiation of Upper-Room Air in Inactivating Airborne Bacterial Spores and Mycobacteria in Full-Scale Studies. *Atmos. Environ.* **2003**, 37 (3), 405–419.
- (45) Nicas, M.; Miller, S. L. A Multi-Zone Model Evaluation of the Efficacy of Upper-Room Air Ultraviolet Germicidal Irradiation. *Appl. Occup. Environ. Hyg.* **1999**, 14 (5), 317–328.
- (46) Lakey, P. S. J.; Won, Y.; Shaw, D.; Østerstrøm, F. F.; Mattila, J.; Reidy, E.; Bottorff, B.; Rosales, C.; Wang, C.; Ampollini, L.; Zhou, S.; Novoselac, A.; Kahan, T. F.; DeCarlo, P. F.; Abbatt, J. P. D.; Stevens, P. S.; Farmer, D. K.; Carslaw, N.; Rim, D.; Shiraiwa, M. Spatial and Temporal Scales of Variability for Indoor Air Constituents. *Communications Chemistry* **2021**, 4 (1), 110.
- (47) Daisey, J. M.; Angell, W. J.; Apte, M. G. Indoor Air Quality, Ventilation and Health Symptoms in Schools: An Analysis of Existing Information. *Indoor Air* **2003**, 13 (1), 53–64.
- (48) Lee, K.; Vallarino, J.; Dumyahn, T.; Ozkaynak, H.; Spengler, J. D. Ozone Decay Rates in Residences. *J. Air Waste Manage. Assoc.* **1999**, 49 (10), 1238–1244.
- (49) Buonanno, G.; Morawska, L.; Stabile, L. Quantitative Assessment of the Risk of Airborne Transmission of SARS-CoV-2 Infection: Prospective and Retrospective Applications. *Environ. Int.* **2020**, 145, 106112.
- (50) Riley, E. C.; Murphy, G.; Riley, R. L. Airborne Spread of Measles in a Suburban Elementary School. *Am. J. Epidemiol.* **1978**, 107 (5), 421–432.
- (51) EPA. Chapter 6—Inhalation Rates. In *Exposure Factors Handbook*; U.S. Environmental Protection Agency, 2011.
- (52) Peng, Z.; Jimenez, J. L. Exhaled CO₂ as a COVID-19 Infection Risk Proxy for Different Indoor Environments and Activities. *Environmental Science & Technology Letters* **2021**, 8 (5), 392–397.
- (53) Ren, X.; Olson, J. R.; Crawford, J. H.; Brune, W. H.; Mao, J.; Long, R. B.; Chen, Z.; Chen, G.; Avery, M. A.; Sachse, G. W.; Barrick, J. D.; Diskin, G. S.; Huey, L. G.; Fried, A.; Cohen, R. C.; Heikes, B.; Wennberg, P. O.; Singh, H. B.; Blake, D. R.; Shetter, R. E. HO_xchemistry during INTEx-A 2004: Observation, Model Calculation, and Comparison with Previous Studies. *J. Geophys. Res.* **2008**, 113 (D5). <https://doi.org/10.1029/2007jd009166>.
- (54) Peng, Z.; Lee-Taylor, J.; Orlando, J. J.; Tyndall, G. S.; Jimenez, J. L. Organic Peroxy Radical Chemistry in Oxidation Flow Reactors and Environmental Chambers and Their Atmospheric Relevance. *Atmos. Chem. Phys.* **2019**, 19 (2), 813–834.
- (55) Pagonis, D.; Algrim, L. B.; Price, D. J.; Day, D. A.; Handschy, A. V.; Stark, H.; Miller, S. L.; de Gouw, J. A.; Jimenez, J. L.; Ziemann, P. J. Autoxidation of Limonene Emitted in a University Art Museum. *Environ. Sci. Technol. Lett.* **2019**, 6 (9), 520–524.

- (56) Shrivastava, M.; Cappa, C. D.; Fan, J.; Goldstein, A. H.; Guenther, A. B.; Jimenez, J. L.; Kuang, C.; Laskin, A.; Martin, S. T.; Ng, N. L.; Petaja, T.; Pierce, J. R.; Rasch, P. J.; Roldin, P.; Seinfeld, J. H.; Shilling, J.; Smith, J. N.; Thornton, J. A.; Volkamer, R.; Wang, J.; Worsnop, D. R.; Zaveri, R. A.; Zelenyuk, A.; Zhang, Q. Recent Advances in Understanding Secondary Organic Aerosol: Implications for Global Climate Forcing. *Rev. Geophys.* **2017**, 55 (2), 509–559.
- (57) Hhs, U. S. Agency for Toxic Substances and Disease Registry Minimal Risk Levels [WWW Document]. URL <https://www.atsdr.cdc.gov/about/index.html> (accessed 12. 18. 18) **2018**.
- (58) Whalen, J. J. *Environmental Control for Tuberculosis; Basic Upper-Room Ultraviolet Germicidal Irradiation Guidelines for Healthcare Settings Guide*; (NIOSH) 2009-105; 2009.
- (59) Riley, R. L.; Permutt, S. Room Air Disinfection by Ultraviolet Irradiation of Upper Air. Air Mixing and Germicidal Effectiveness. *Arch. Environ. Health* **1971**, 22 (2), 208–219.
- (60) Morawska, L.; Tang, J. W.; Bahnfleth, W.; Bluyssen, P. M.; Boerstra, A.; Buonanno, G.; Cao, J.; Dancer, S.; Floto, A.; Franchimon, F.; Haworth, C.; Hogeling, J.; Isaxon, C.; Jimenez, J. L.; Kurnitski, J.; Li, Y.; Loomans, M.; Marks, G.; Marr, L. C.; Mazzearella, L.; Melikov, A. K.; Miller, S.; Milton, D. K.; Nazaroff, W.; Nielsen, P. V.; Noakes, C.; Peccia, J.; Querol, X.; Sekhar, C.; Seppänen, O.; Tanabe, S.-I.; Tellier, R.; Tham, K. W.; Wargocki, P.; Wierzbicka, A.; Yao, M. How Can Airborne Transmission of COVID-19 Indoors Be Minimised? *Environ. Int.* **2020**, 142, 105832.
- (61) Lee, P.; Davidson, J. Evaluation of Activated Carbon Filters for Removal of Ozone at the PPB Level. *Am. Ind. Hyg. Assoc. J.* **1999**, 60 (5), 589–600.
- (62) Mochida, I.; Korai, Y.; Shirahama, M.; Kawano, S.; Hada, T.; Seo, Y.; Yoshikawa, M.; Yasutake, A. Removal of SO_x and NO_x over Activated Carbon Fibers. *Carbon N. Y.* **2000**, 38 (2), 227–239.